JCTC Journal of Chemical Theory and Computation

Coarse-Grained MD Simulations and Protein−Protein Interactions: The Cohesin−Dockerin System

Benjamin A. Hall and Mark S. P. Sansom*

Department of Biochemistry & Oxford Centre for Integrative Systems Biology, University of Oxford, South Parks Road, Oxford OX1 3QU, U.K.

Received March 25, 2009

Abstract: Coarse-grained molecular dynamics (CG-MD) may be applied as part of a multiscale modeling approach to protein−protein interactions. The cohesin−dockerin interaction provides a valuable test system for evaluation of the use of CG-MD, as structural (X-ray) data indicate a dual binding mode for the cohesin−dockerin pair. CG-MD simulations (of 5 μs duration) of the association of cohesin and dockerin identify two distinct binding modes, which resemble those observed in X-ray structures. For each binding mode, ca. 80% of interfacial residues are predicted correctly. Furthermore, each of the binding modes identified by CG-MD is conformationally stable when converted to an atomistic model and used as the basis of a conventional atomistic MD simulation of duration 20 ns.

Introduction

Coarse-grained molecular dynamics (CG-MD) simulations have been used in a number of simulation studies of lipid bilayers and related systems.[1−4] More recently they have been extended with some success to simple membrane−peptide and membrane−protein systems.[5,6] The latter studies have included simulations of protein−protein interactions within membranes.[7,8] It is therefore of interest to explore whether such approaches can be applied to protein/protein interactions *outside* of a membrane environment. This is of relevance both in the context of computational studies of protein docking in general[9−11] and also in the context of wishing to develop multiscale biomolecular simulations[12−14] to study protein complexes.

The cohesin−dockerin system[15] provides a good test case for the application of CG-MD to protein−protein interactions, as crystallographic studies indicate a degree of complexity in the interaction, with the possibility of a dual binding mode.[16] This complex, which forms a key recognition element of the cellulosome,[17] provides a model system for macromolecular assembly. Subunits within the larger complex recognize each other through the interaction of type 1 dockerins and various cohesins. X-ray structures of the cohesin−dockerin complex from *Clostridium thermocellum*[15,16] suggest a role for plasticity in the protein−protein interaction. Comparisons of two structures indicate that the complex can be seen to bind in two modes, related to one another by a ∼180° rotation. The interactions defined in the crystal structures are composed of both packing of hydrophobic residues and of a hydrogen bonding network along two α-helices (related by a pseudo-2-fold axis) on the dockerin binding face.

Here we describe the application of CG-MD simulations to the encounter and interactions between dockerin and cohesin. These simulations are compared for the wild-type protein and for a mutant of dockerin[15,16] at the interaction interface. The CG-MD simulations of dockerin/cohesin encounter are also compared with those with simulations of the intact complex as seen in the two X-ray structures. We show that CG-MD is able to reproduce key aspects of the interaction between these two proteins. We also explore the conversion of a CG-MD generated model of the cohesin−dockerin complex to an atomistic representation, exemplifying a multiscale approach[14] to simulation of protein−protein interactions.

Methods

Coarse-Grained Simulations. Coarse-grain models of proteins were generated from their X-ray structures using procedures described previously[6,18] using a modified version

* Corresponding author phone: +44 1865 613306; fax: +44 1865 613238; e-mail: mark.sansom@bioch.ox.ac.uk.

10.1021/ct900140w CCC: $40.75
Published on Web 08/20/2009

Table 1. Summary of Simulations

simulation[a]	protein coordinate source	starting configuration
WT_{dock}	1OHZ	subunits separated
$WT_{X\text{-}ray}$	1OHZ	crystal structure
MUT_{dock}	2CCL	subunits separated
$MUT_{X\text{-}ray}$	2CCL	crystal structure

[a] For each simulation setup, four individual simulations of duration 5 μs were performed, differing in their initial random velocities.

of procedure described by Marrink and colleagues.[2] Briefly, a 4:1 mapping of non-H atoms to coarse grain particles is used. Interparticle interactions are modeled as Lennard-Jones interactions between 4 classes of particles (2 of which are divided into subtypes to reflect hydrogen bonding). Electrostatics interactions are treated Coulombically. The protein fold is maintained using an elastic network model[19] with a cutoff between backbone particles of 7 Å and a force constant of 10 kJ mol^{-1} $Å^{-2}$. Lennard-Jones interactions were shifted to zero between 9 and 12 Å, and electrostatic interactions were shifted to zero between 0 and 12 Å. CG simulations were performed with GROMACS 3.3.1. (www.gromacs.org).[20]

To perform a docking simulation the two binding partners (cohesin and dockerin) in a cubic simulation box (length 100 Å) at a distance of 40 Å apart, equal to the sum of their respective radii of gyrations multiplied by 1.2, plus the cutoff distance for interactions. The proteins were randomly oriented with respect to one another, and four separate simulations were performed, each of duration 5 μs. The system temperature was 348 K, maintained using a Berendsen thermostat[21] ($\tau_T = 1$ ps). Pressure was coupled with a Berendsen barostat at 1 bar ($\tau_P = 1$ ps). Simulations of the 1OHZ and 2CCL structures were performed from their crystal structure with the same representation.

Atomistic Simulations. Following a CG simulation, 20 representative structures (based on cluster analysis) from the last 0.5 μs in thesis of a trajectory were used along with the initial X-ray structures of component proteins from 1OHZ to generate 25 structures using MODELER (http://www.salilab.org/modeller/).[22] The resultant model structure of the cohesin−dockerin complex was used as the starting point for a conventional atomistic MD simulation using GROMACS and the GROMOS96 force field.[23] The structure was solvated with SPC water (10,500 waters in a (70 Å)^3 simulation box) and counterions, energy minimized for 100 steps (using the steepest descent algorithm), and equilibrated by a 0.5 ns protein position-restrained) simulation followed by a 20 ns unrestrained simulation. The temperature was 300 K and was coupled using a Berendsen thermostat ($\tau_T = 0.1$ ps). Long range electrostatic interactions were treated with particle mesh Ewald.[24] Analysis of simulations and visualization used VMD.[25]

Results

Progress of CG-MD Simulations. Four sets of simulations were performed, as summarized in Table 1. These correspond to the wild-type (WT; PDB id 1OHZ) and mutant (MUT; PDB id 2CCL) structures. Note that the mutant has two changes of side chain (S45A, T46A) on the surface of one of the interaction site helices (α3) of dockerin, resulting in a change in the mode of interaction within the crystal structure.[16] For each of WT and MUT, simulations were performed starting with either the two subunits separated (and in random orientations relative to one another) or with the two subunits in the complex found in their respective crystal structure.

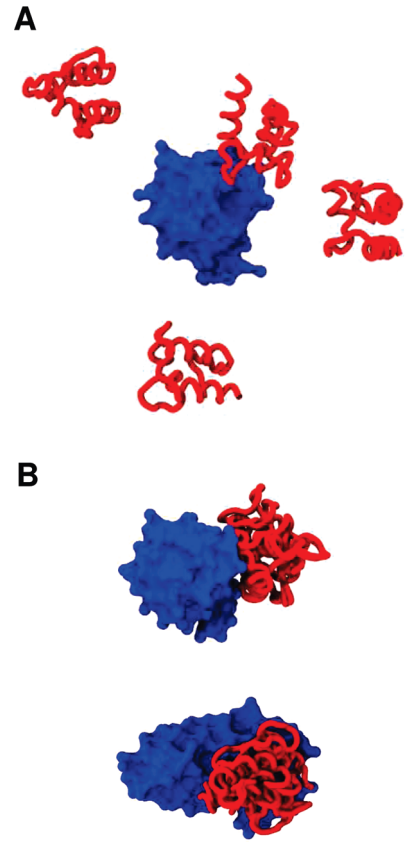

Figure 1. Progress of the four CG-MD simulations (WT_{dock}) of the cohesin−dockerin interaction. **A** Initial positions of dockerin molecules (red; Cα trace) relative to cohesin (blue; surface). **B** Two perpendicular views of the final (5 μs) positions of the four dockerin molecules (red; superimposed structures, one from each simulation) relative to cohesin (blue).

The start and end configurations of four 5 μs CG-MD simulations of the WT_{dock} cohesin−dockerin encounter are shown in Figure 1. In each case the dockerin finds the same 'site' on the surface of the cohesin molecule. The cohesin usually attaches to this site within 100 ns of simulation time, and the final binding mode is achieved within ∼1 μs (although it should be noted that the scaling of CG time to real time is somewhat uncertain[2,18]). It is evident that in all four simulations the same broadly defined 'site' on the cohesin is occupied by the dockerin. This is the same site of interaction as is seen in both of the X-ray structures (1OHZ and 2CCL) which define the two binding modes of dockerin on cohesin.[16] Indeed in comparable simulations of the encounter of cohesin with the mutated dockerin (MUT_{dock})

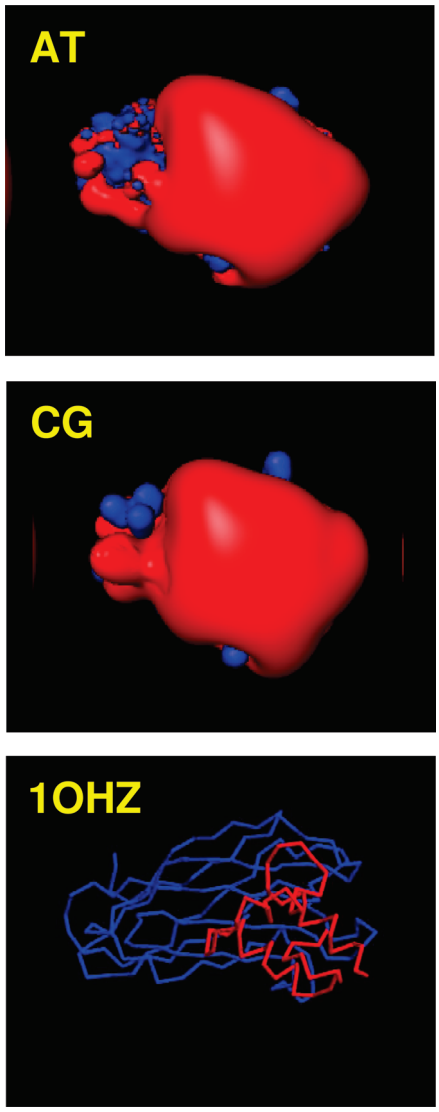

Figure 2. Isopotential surfaces (contours at ±3 kT, red = negative, blue = positive) from Poisson−Boltzmann electrostatics calculations (using APBS[26]) for atomistic (AT) and coarse-grained (CG) models of cohesin. A Cα trace representation of the cohesin/dockerin complex (1OHZ) in approximately the same orientation is shown for reference.

the same interaction site is seen in the two simulations for which a complex is formed within 5 μs (see below for further details).

Comparison of surface electrostatic potentials (calculated using APBS;[26] Figure 2) from CG models of cohesin and dockerin with those from the corresponding all atom structures reveals that the coarse-graining does not qualitatively alter the overall pattern of protein surface electrostatics between the AT and the CG model. The binding surface of cohesin has a distinct region of negative potential, which interacts with a complementary positive surface on dockerin.

The nature of the protein−protein interaction surface yielded by the CG-MD docking can be examined in more detail by calculation of the fraction of correct residues in the interface (F*IR* - see Table 2 for details) and by examination in more detail of the patterns of contact residues (Figure 3).

Table 2. Fraction of Residues in the Interface for WT_{dock} Simulations[a]

comparison structure	protein	F*IR*				
		Sim1	Sim2	Sim3	Sim4	mean (SD)
1OHZ	cohesin	0.85	0.87	0.87	0.90	0.87 (0.02)
	dockerin	0.57	0.84	0.61	0.86	0.72 (0.15)
2CCL	cohesin	0.76	0.76	0.74	0.80	0.77 (0.03)
	dockerin	0.51	0.35	0.50	0.38	0.44 (0.08)

[a] F*IR* = (number of correct residues in interface)/(total number of residues in interface). The values given are averages over the last microsecond of each simulation. Residues within the interface are defined using a cutoff distance between partner proteins of 7.5 Å. The 'correct' residues are scored according to either the 1OHZ or 2CCL structures of the cohesin−dockerin interface.

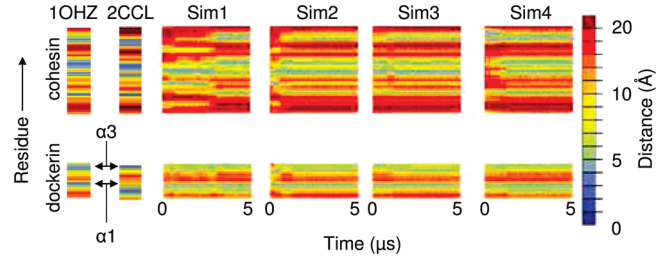

Figure 3. Fingerprint analysis of the time dependence of the cohesin−dockerin contacts a function of time for the WT_{dock} simulations. Blues are closer contacts, reds more distant. The corresponding fingerprints of the contacts in the two crystal structures (1OHZ and 2CLL) are given to the left of the time dependent fingerprints of the four CG-MD simulations. (Interaction fingerprints are calculated from the shortest distance between a residue in one binding protein and any residue in its partner. This is plotted against time for each simulation.)

The 'correct' residues for the cohesin−dockerin interface can be defined using either the WT (1OHZ) or MUT (2CCL) structures (which have very similar residues in their interfaces). Thus, for each simulation and protein two F*IR* values can be defined (Table 1). It should be noted that when evaluating F*IR* values for CG models the reduction in particle number coupled with the increase in particle size in coarse-graining requires a cutoff of 7.5 Å to be used, rather than a more typical value of e.g. 5 Å used to evaluate inter-residue contacts in an AT model (see Supporting Information, Figure S1). From these it can be seen that scoring against either X-ray structure, between 80% and 90% of the cohesin interface residues are present in the CG-MD generated structures from the WT_{dock} simulations. For dockerin, between ∼50% (scored against 2CCL) and ∼75% (scored against 1OHZ) of the correct interfacial residues are present in these CG-MD simulations. rmsd analyses and clustering reinforces the identification of 2 distinct end points in the simulations, resembling the two crystal conformations.

The patterns of interacting residues can be identified through the course of the simulation via residue contact 'fingerprints' (Figure 3). Examination of these fingerprints for the two X-ray structures (1OHZ and 2CCL) shows that similar residues are involved in both modes of binding (but see below). Examination of the time-dependent simulations reveals some changes in the initial contact pattern over the first 1−2 μs of a simulation, followed by a pattern of interaction which remains constant until the end of the

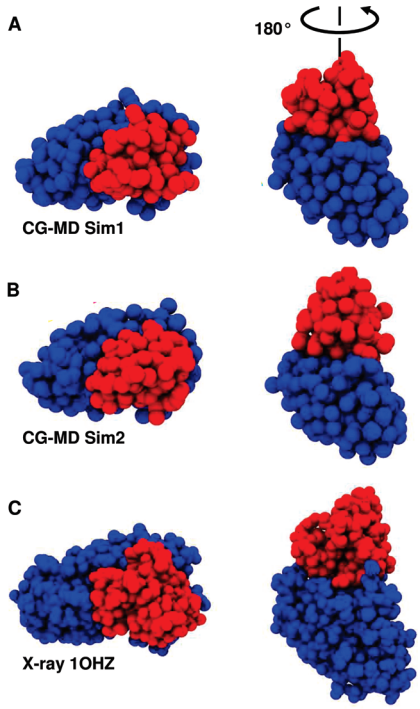

Figure 4. Identification of alternative models of interactions. Orthogonal views of the cohesin (blue)−dockerin (red) complex from **A** CG-MD WT_{dock} Sim1, **B** CG-MD WT_{dock} Sim2, and **C** X-ray structure 1OHZ. In **A** the ∼180° rotation about an axis perpendicular to the protein−protein interface which relates a 1OHZ-like to a 2CCL-like complex is indicated.

simulation. The final patterns are similar for the four WT_{dock} simulations (and in particular the main contacts are for the α1 and α3 helices of dockerin) and in turn resemble those in the two X-ray structures. The MUT_{dock} simulations match the two X-ray structures in two of the four simulations, in one simulation matching the 2CCL structure better than in any of the WT_{dock} simulations (as revealed by the rmsd values, see Supporting Information, Figure S3B). The other two MUT_{dock} simulations yielded non-native binding interactions.

Two Interaction Modes. Visualization of the structure yielded by CG-MD WT_{dock} reveals a complication. There are two distinct orientations of the dockerin molecule while interacting with the same site on the cohesin. These correspond to an ∼180° rotation of the dockerin relative to cohesin about an axis normal to the protein−protein interface (compare Figure 4A and B). This can be compared to the two X-ray structures (1OHZ and 2CCL) which are related by a similar transformation, reflecting the approximate 2-fold symmetry of the structure of dockerin, which relates helices α1 and α3, i.e. the two helices which interact with the cohesin binding site. Again, simple visualization suggests that the CG-MD structures can be classified as either 1OHZ-like (Sim1 and Sim3, Figure 5A) or 2CCL-like (Sim2 and Sim4, Figure 5B) in terms of the orientation of the dockerin relative to the cohesin, even though both modeled (and indeed X-ray) complexes share the same interfacial residues. Interestingly, in the two mutant simulations (MUT_{dock}) which yielded complexes, Sim4 gave a 1OHZ-like structure and Sim1 a 2CCL-like structure, whereas the remaining pair gave non-native docks (see Supporting Information, Figure S3).

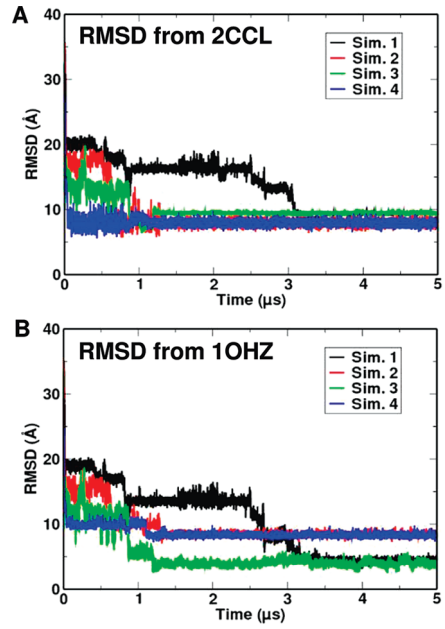

Figure 5. Comparison with X-ray structures. For each of the four WT_{dock} self-assembly simulations, Cα RMSDs are evaluated relative to the two crystal structures, namely **A** 2CCL and **B** 1OHZ. From this it can be seen that Sim1 and Sim3 yield structures close to 1OHZ, while Sim2 and Sim4 yield structures closer to 2CCL.

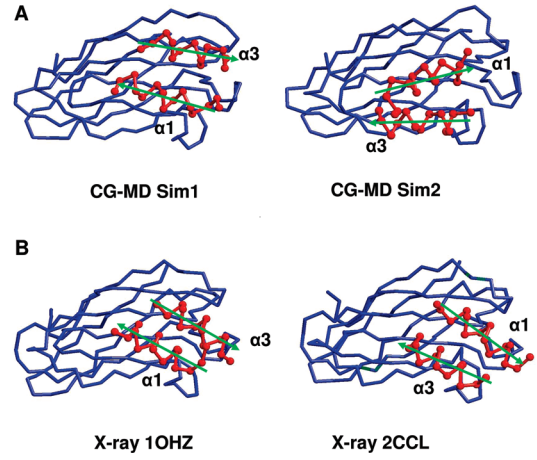

Figure 6. **A** Final (5 μs) structure of the cohesin (blue)-dockerin (red) complex from CG-MD simulations WT_{dock} Sim1 and Sim2, showing the Cα trace of the complete cohesin domain but just the two interaction helices (α1 and α3) of the dockerin domain.. The directions of the two interaction helices are shown by green arrows. **B** Equivalent diagrams for the 1OHZ and 2CCL X-ray structures of the complex.

This can be seen more clearly if one focuses on just the α1 and α3 interaction helices of dockerin (Figure 6). Comparison of e.g. the end structures of simulations WT_{dock} Sim1 and Sim2 reveals two different orientations of α1 and α3 on the cohesin binding site. This closely mirrors the similar two orientations seen in the wild-type (1OHZ) and mutant (S45A-T46A, in α3; 2CCL) structures. Thus it would seem that not only is CG-MD able to predict the correct binding interface for the cohesin−dockerin interaction but also is able to reproduce the dual binding mode revealed by comparison of a wild-type and mutant crystal structure.

This may be analyzed in more detail via calculation of the Cα particle root-mean-square deviations (RMSDs) for the WT_{dock} simulations relative to the two possible structures of the complex (i.e., 1OHZ and 2CCL; Figure 5). Those simulations (Sim1 and Sim3) which converge to a 1OHZ-like structure are within 5 Å of the original 1OHZ crystal structure. They also give mean F_{NAT} values of 0.21 and 0.26 over the last microsecond (compared to the Sim2 and Sim4, which give 0.07; all calculated with a 7.5 Å cutoff). This is comparable to the drift from this structure seen in the $1OHZ_{Xray}$ simulation (see Supporting InformationFigure S2), which corresponds to the drift observed in simulations starting from the crystal structure. Likewise, the rmsd of the 2CCL-like structures is also similar to that observed in the $2CCL_{Xray}$ simulations. In addition, cluster analysis supports the convergence of Sim1 and Sim3 to a 1OHZ-like common structure and of Sim2 and Sim4 to a 2CCL-like common structure (data not shown).

Atomistic MD Simulations. In order to facilitate further comparison with the X-ray structures, and also to explore the (short time scale) conformational stability of the model complexes generated by CG-MD, the latter were converted to atomistic models and used as the starting point for short (20 ns) conventional MD simulations. Two CG complexes were used as the starting point for AT-MD simulations. One (from WT_{dock} Sim1) was a 1OHZ-like complex; the other (from WT_{dock} Sim2) was a 2CCL-like complex, as discussed above. We note that AT simulations have been used previously to refine and explore flexible docking of proteins and that in these studies some rearrangements in protein−protein interactions were seen on a nanosecond time scale.[27] However, we realize that large scale rearrangements of docked structures are unlikely to occur on a 20 ns time scale. Thus, the AT-MD simulations largely serve to 'relax' the CG-MD generated models.

The individual proteins were conformationally stable (over 20 ns) in both AT-MD simulations. Thus, for the Sim1 complex, the Cα RMSDs of the individual proteins are ∼2 Å for the cohesin and ∼3 Å for the dockerin (Figure 7A). Similar behavior is observed for the Sim2 derived structure. Furthermore, the two Ca^{2+} ions bound by the EF hands of the dockerin remained stably bound over the course of the 20 ns. (Note that these ions were not modeled explicitly in the CG representation). Thus, the individual proteins remain conformationally stable after the CG to AT conversion.

It is also of interest to examine the energetic relaxation (Figure 7B) of the complex over the course of the AT-MD simulation. From this analysis it can be seen that, as anticipated, there is a fast initial relaxation (over ∼2 ns), but no further major changes. This suggests 'local' relaxation of the CG-generated model but no substantial changes in conformation over the course of the AT-MD simulation.

By comparing the Cα rmsd of the model complex vs the two X-ray structures (Figure 7C) it can be seen that the structure of the complex from Sim1 compares well with the 1OHZ X-ray structure, with an overall Cα rmsd of ∼3 Å. This does not change significantly over the course of the AT-MD simulation and is within the drift typically observed in atomistic simulations from *crystal* structures. By way of

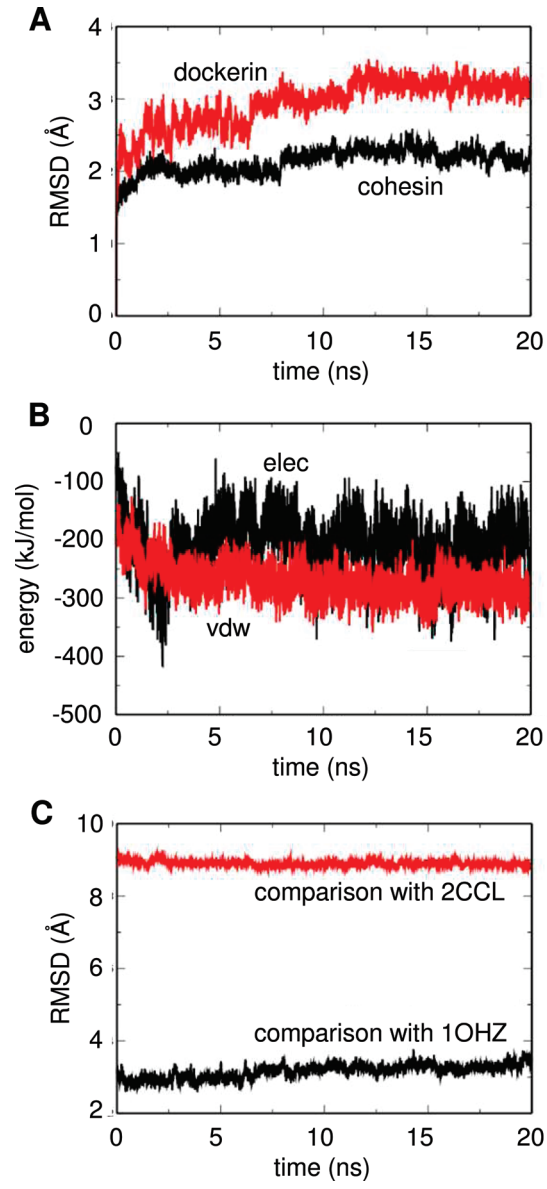

Figure 7. Atomistic simulation of the cohesin−dockerin complex generated from CG-MD WT_{dock} Sim1. **A** Cα RMSDs relative to starting model for cohesin and dockerin separately (fitted on cohesin). **B** Potential energy of interaction vs time. **C** Cα RMSDs of the complete complex vs the two X-ray structures vs time.

comparison, the rmsd vs 2CCL is ∼9 Å, supporting our classification of Sim1 having yielded a 1OHZ-like complex. For Sim2 the rmsd vs 1OHZ is 8 Å and that vs 2CCL is ∼6 Å. Again there is little change over the course of 20 ns AT-MD. Thus, we may conclude that although conversion to atomistic resolution and subsequent MD simulation allows some local relaxation of the proteins and there interface, as one might expect no substantial changes are seen on this relatively short time scale.

One may also analyze the AT-MD simulations via the metrics used in e.g. the CAPRI protein docking assessment.[9] F*NAT* is defined as the (number of correct contacts)/(number of contacts in the crystal) assessed using a 5 Å cutoff. For the AT-MD simulation based on Sim1 F*NAT* (compared to 1OHZ) is ∼0.25. The F*IR* values are essentially unchanged from the CG-MD simulations. Thus, CG-MD has generated

an acceptable structure of the 1OHZ-like complex. For Sim2 the comparison is not as promising - its F*NAT* is <0.1 (compared to 2CCL), and the F*IR* values are again the same as in the CG-MD model. However, one should remember that the 2CCL X-ray structure is of a mutant rather than wild-type protein.

Discussion

In this study we demonstrate the application of CG-MD to a complex protein−protein interaction problem involving a dual binding mode of the two proteins. Within the limitations of a CG representation, the approach is successful in revealing both binding modes[16,28] of the cohesin−dockerin complex.

A multiscale approach (in which the CG model of the complex was converted to an atomistic model) confirmed the conformational stability of the resultant complex, albeit in relatively short time scale MD simulations. This multiscale strategy has some potential for modeling protein−protein interactions. The CG model allows protein flexibility to be addressed efficiently, while conversion to an atomistic model enables validation and refinement of the resultant structures. Further exploration of this method with a wider set of test cases (Hall and Sansom, unpublished results) will enable refinement of the approach e.g. via refinement of CG models for proteins.[29]

It is of interest that CG-MD predicted the 1OHZ binding mode better than the 2CCL mode. However, we note that in the experimental studies a mutation of key interaction residues (S45A-T46A, in the α3 helix of dockerin) was required to promote the 2CCL binding mode. In particular, the 2CCL-like structure yielded by CG-MD is to be related to the (mutant) crystal structure by a ∼10 Å translation. Of course, the crystal structure also represents the protein complex at a temperature of 110 K, and it is possible that the interaction is more plastic in the wild-type under physiological conditions. However, a similar orientation has been observed in the 2CCL-like mode seen in the A47S/F48T mutant of the *Cl. cellulolyticum* (PDB id 2 VN5) cohesin−dockerin complex.[28] CG-MD simulations of the 2CCL crystal structure (MUT_{Xray}) do indicate a somewhat 'softer' interface for the S45A, T46A dockerin mutant, clustering less clearly than the $WT_{X\text{-}ray}$ simulation and drifting further away from the crystal structure (see Supporting Information, Figure S2).

Protein−protein interactions in general, and the cohesin−dockerin interaction in particular, have been studied using a wide range of computational approaches to protein−protein docking (see refs 10 and 11 for recent reviews), and indeed the 1OHZ cohesin−dockerin complex was used in the CAPRI (round 4) assessment of protein docking (http://www.ebi.ac.uk/msd-srv/capri/capri.html) both as a direct protein−protein dock (T12) and as dock between the experimental cohesin structure and a homology model of dockerin (T12).[10]

Our results compare favorably with those of a number of protein docking algorithms applied to 1OHZ in round 4 of CAPRI, including ZDOCK,[30] *Hex*,[31] and HADDOCK.[32] Thus ZDOCK yielded a F*IR* of 0.84 and HADDOCK of ∼0.8 compared to ∼0.8 for CG-MD (see above). Interestingly, it was noted for e.g. HADDOCK that several predicted docks were for a ∼180° rotated (i.e., 2CCL-like) interaction of the two proteins. Scoring of these docking methods against the 2CCL interaction mode have not been reported.

In summary, we have described CG-MD as an extension of the use of MD simulations for docking (e.g., refs 27 and 33), related to a number of other coarse-grained approaches to study protein−protein interactions (e.g., refs 34 and 35). It will be of interest to further develop the multiscale approach applied here to the cohesin−dockerin interaction to a range of other protein−protein interactions, perhaps by combining high throughput approaches (to improve sampling) with treatment of the initial protein−protein encounter by e.g. Brownian dynamics simulation[36] followed by CG- and AT-MD.

Acknowledgment. This work was supported by grants from the BBSRC and MRC. Our thanks to Oliver Beckstein and Peter Bond for helpful discussions.

Supporting Information Available: Figures S1−S3. This material is available free of charge via the Internet at http://pubs.acs.org.

References

(1) Shelley, J. C.; Shelley, M. Y.; Reeder, R. C.; Bandyopadhyay, S.; Klein, M. L. A coarse grain model for phospholipid simulations. *J. Phys. Chem. B* **2001**, *105*, 4464–4470.

(2) Marrink, S. J.; de Vries, A. H.; Mark, A. E. Coarse grained model for semiquantitative lipid simulations. *J. Phys. Chem. B* **2004**, *108*, 750–760.

(3) Nielsen, S. O.; Lopez, C. F.; Srinivas, G.; Klein, M. L. Coarse grain models and the computer simulation of soft materials. *J. Phys.: Condens. Matter* **2004**, *16*, R481–R512.

(4) Stevens, M. J. Coarse-grained simulations of lipid bilayers. *J. Chem. Phys.* **2004**, *121*, 11942–11948.

(5) Lindahl, E.; Sansom, M. S. P. Membrane proteins: molecular dynamics simulations. *Curr. Opin. Struct. Biol.* **2008**, *18*, 425–431.

(6) Bond, P. J.; Holyoake, J.; Ivetac, A.; Khalid, S.; Sansom, M. S. P. Coarse-grained molecular dynamics simulations of membrane proteins and peptides. *J. Struct. Biol.* **2007**, *157*, 593–605.

(7) Periole, X.; Huber, T.; Marrink, S. J.; Sakmar, T. P. G protein-coupled receptors self-assemble in dynamics simulations of model bilayers. *J. Am. Chem. Soc.* **2007**, *129*, 10126–10132.

(8) Psachoulia, E.; Bond, P. J.; Fowler, P. W.; Sansom, M. S. P. Helix-helix interactions in membrane proteins: coarse grained simulations of glycophorin helix dimerization. *Biochemistry* **2008**, *47*, 10503–105012.

(9) Janin, J.; Henrick, K.; Moult, J.; Ten Eyck, L.; Sternberg, M. J. E.; Vajda, S.; Vakser, I.; Wodak, S. J. CAPRI: a Critical Assessment of PRedicted Interactions. *Proteins: Struct., Funct., Bioinf.* **2003**, *52*, 2–9.

(10) Gray, J. J. High-resolution protein-protein docking. *Curr. Opin. Struct. Biol.* **2006**, *16*, 183–193.

(11) Bonvin, A. M. J. J. Flexible protein-protein docking. *Curr. Opin. Struct. Biol.* **2006**, *16*, 194–200.

(12) Izvekov, S.; Voth, G. A. A multiscale coarse-graining method for biomolecular systems. *J. Phys. Chem. B* **2005**, *109*, 2469–2473.

(13) Ayton, G. A.; Noid, W. G.; Voth, G. A. Multiscale modeling of biomolecular systems: in serial and in parallel. *Curr. Opin. Struct. Biol.* **2007**, *17*, 192–198.

(14) Sherwood, P.; Brooks, B. R.; Sansom, M. S. P. Multiscale methods for macromolecular simulations. *Curr. Opin. Struct. Biol.* **2008**, *18*, 630–640.

(15) Carvalho, A. L.; Dias, F. M. V.; Prates, J. A. M.; Nagy, T.; Gilbert, H. J.; Davies, G. J.; Ferreira, L. M. A.; Romao, M. J.; Fontes, C. Cellulosome assembly revealed by the crystal structure of the cohesin−dockerin complex. *Proc. Natl. Acad. Sci. U.S.A.* **2003**, *100*, 13809–13814.

(16) Carvalho, A. L.; Dias, F. M. V.; Nagy, T.; Prates, J. A. M.; Proctor, M. R.; Smith, N.; Bayer, E. A.; Davies, G. J.; Ferreira, L. M. A.; Romao, M. J.; Fontes, C.; Gilbert, H. J. Evidence for a dual binding mode of dockerin modules to cohesins. *Proc. Natl. Acad. Sci. U.S.A.* **2007**, *104*, 3089–3094.

(17) Doi, R. H.; Kosugi, A. Cellulosomes: plant-cell-wall-degrading enzyme complexes. *Nature Rev. Microbiol.* **2004**, *2*, 541–551.

(18) Bond, P. J.; Sansom, M. S. P. Insertion and assembly of membrane proteins via simulation. *J. Am. Chem. Soc.* **2006**, *128*, 2697–2704.

(19) Atilgan, A. R.; Durell, S. R.; Jernigan, R. L.; Demirel, M. C.; Keskin, O.; Bahar, I. Anisotropy of fluctuation dynamics of proteins with an elastic network model. *Biophys. J.* **2001**, *80*, 505–515.

(20) Lindahl, E.; Hess, B.; van der Spoel, D. GROMACS 3.0: a package for molecular simulation and trajectory analysis. *J. Mol. Model.* **2001**, *7*, 306–317.

(21) Berendsen, H. J. C.; Postma, J. P. M.; van Gunsteren, W. F.; DiNola, A.; Haak, J. R. Molecular dynamics with coupling to an external bath. *J. Chem. Phys.* **1984**, *81*, 3684–3690.

(22) Sali, A.; Blundell, T. L. Comparative protein modeling by satisfaction of spatial restraints. *J. Mol. Biol.* **1993**, *234*, 779–815.

(23) Scott, W. R. P.; Hunenberger, P. H.; Tironi, I. G.; Mark, A. E.; Billeter, S. R.; Fennen, J.; Torda, A. E.; Huber, T.; Kruger, P.; van Gunsteren, W. F. The GROMOS biomolecular simulation program package. *J. Phys. Chem. A* **1999**, *103*, 3596–3607.

(24) Darden, T.; York, D.; Pedersen, L. Particle mesh Ewald - an N.log(N) method for Ewald sums in large systems. *J. Chem. Phys.* **1993**, *98*, 10089–10092.

(25) Humphrey, W.; Dalke, A.; Schulten, K. VMD - Visual Molecular Dynamics. *J. Mol. Graph.* 1996*14*, 33–38.

(26) Baker, N. A.; Sept, D.; Joseph, S.; Holst, M. J.; McCammon, J. A. Electrostatics of nanosystems: application to microtubules and the ribosome. *Proc. Natl. Acad. Sci. U.S.A.* **2001**, *98*, 10037–10041.

(27) Wang, T.; Wade, R. C. Implicit solvent models for flexible protein-protein docking by molecular dynamics simulation. *Proteins: Struct., Funct., Bioinf.* **2003**, *50*, 158–169.

(28) Pinheiro, B. A.; Proctor, M. R.; Martinez-Fleites, C.; Prates, J. A. M.; Money, V. A.; Davies, G. J.; Bayer, E. A.; Fontes, C.; Fierobe, H. P.; Gilbert, H. J. The *Clostridium cellulolyticum* dockerin displays a dual binding mode for its cohesin partner. *J. Biol. Chem.* **2008**, *283*, 18422–18430.

(29) Monticelli, L.; Kandasamy, S. K.; Periole, X.; Larson, R. G.; Tieleman, D. P.; Marrink, S. J. The MARTINI coarse grained force field: extension to proteins. *J. Chem. Theory Comput.* **2008**, *4*, 819–834.

(30) Wiehe, K.; Pierce, B.; Mintseris, J.; Tong, W. W.; Anderson, R.; Chen, R.; Weng, Z. ZDOCK and RDOCK performance in CAPRI rounds 3, 4, and 5. *Proteins: Struct., Funct., Bioinf.* **2005**, *60*, 207–213.

(31) Mustard, D.; Ritchie, D. W. Docking essential dynamics eigenstructures. *Proteins: Struct., Funct., Bioinf.* **2005**, *60*, 269–274.

(32) van Dijk, A. D. J.; de Vries, S. J.; Dominguez, C.; Chen, H.; Zhou, H. X.; Bonvin, A. Data-driven docking: HADDOCK's adventures in CAPRI. *Proteins: Struct., Funct., Bioinf.* **2005**, *60*, 232–238.

(33) Smith, G. R.; Fitzjohn, P. W.; Page, C. S.; Bates, P. A. Incorporation of flexibility into rigid-body docking: Applications in rounds 3−5 of CAPRI. *Proteins: Struct., Funct., Bioinf.* **2005**, *60*, 263–268.

(34) Zacharias, M. ATTRACT: Protein-protein docking in CAPRI using a reduced protein model. *Proteins: Struct., Funct., Bioinf.* **2005**, *60*, 252–256.

(35) Basdevant, N.; Borgis, D.; Ha-Doung, T. A coarse-grained protein-protein potential derived from an all-atom force field. *J. Phys. Chem. B* **2007**, *111*, 9390–9399.

(36) Spaar, A.; Dammer, C.; Gabdoulline, R. R.; Wade, R. C.; Helms, V. Diffusional encounter of barnase and barstar. *Biophys. J.* **2006**, *90*, 1913–1924.

CT900140W